ELSEVIER

Journal of Power Sources 102 (2001) 55–59

JOURNAL OF POWER SOURCES

www.elsevier.com/locate/jpowsour

Electrochemical properties of $LiMg_yMn_{2-y}O_4$ spinel phases for rechargeable lithium batteries

In-Seong Jeong*, Jong-Uk Kim, Hal-Bon Gu

Department of Electrical Engineering, Chonnam National University, 300 Yongbong-dong, Buk-ku, Kwangju 500-757, South Korea

Received 21 February 2001; accepted 22 March 2001

Abstract

The magnesium-substituted spinel $LiMg_yMn_{2-y}O_4$ ($y = 0.0$, 0.05, 0.08, 0.1, 0.12 and 0.15) is synthesised at 800°C for 36 h in air. Its electrochemical performance is examined in $LiMg_yMn_{2-y}O_4$/Li cells. The initial capacity of the cells is lowered on increasing the Mg content. The charge–discharge capacity of substituted spinels is higher than that of pure spinel, even on the first cycle. The discharge capacity of $LiMg_{0.1}Mn_{1.9}O_4$ on the first and 70th cycles is about 120 and l05 mAh/g, respectively. The cell retains about 88% of the initial capacity at the 70th cycle. Impedance profiles of $LiMg_{0.1}Mn_{1.9}O_4$ are more stable than those of the pure spinel during charge–discharge cycling. The initial charge-transfer resistance and the chemical diffusion coefficients of lithium ions in $LiMg_{0.1}Mn_{1.9}O_4$ are about 70 Ω and 10^{-8} cm^2 s^{-1}, respectively.

Keywords: $LiMn_2O_4$; $LiMg_yMn_{2-y}O_4$; Spinel; Cathode materials; Charge–discharge; Lithium-ion battery

1. Introduction

Lithium-ion batteries using intercalation compounds as the positive electrode (cathode) have been studied extensively. The cathode material plays an important role in the operation of lithium-ion batteries. Among the various intercalation compounds which have been used, spinel $LiMn_2O_4$ [1–3] offers considerable advantages over $LiCoO_2$ [4] and $LiNiO_2$ [5] in terms of high cell voltage, a wide operating temperature and long shelf life with much lower cost. $LiMn_2O_4$ has a lower capacity (compared with $LiCoO_2$), however, it suffers from loss of capacity during cycling. The origin for this capacity loss has not been clearly identified, but several possibilities exist, e.g. reactions between the electrolyte and electrode, structural transformation due to Jahn–Teller distortions in the discharged state, and Mn dissolution through a disproportionate ion reaction [6]. To improve the cycle performance of the spinel phase $LiMn_2O_4$, several research groups have studied the properties of manganese-substituted $LiM_yMn_{2-y}O_4$ (M = Cr, Co, Ni, Fe, etc.) [7,8]. Thackeray and co-workers [6] have pointed out that the substitution of a metal cation for Mn enhances the stability of spinels. In addition, Hosoya et al. [9] have suggested that the improvement of the cycleability refers to stronger M–O bonding of the MO_6 octahedron of partially substituted $LiM_yMn_{2-y}O_4$ (M = Cr, Co, Ni) in comparison with that of M–O in the parent $LiMn_2O_4$.

In spinel $LiMn_2O_4$, Li ions reside in the tetrahedral (8a) sites, Mn ions in the octahedral (16d) sites, and O^{2-}ions in octahedral (32e) sites, respectively [10]. The oxygen ions in the octahedral sites form a closed-packed array in the spinel structure. The tetrahedral (8a) sites share faces with empty octahedral (l6c) sites and thus form 3D spaces. Li ions intercalate or de-intercalate through these spaces during electrochemical reaction.

In this work, stoichiometric spinel phases $LiMg_yMn_{2-y}O_4$ are prepared to improve the electrochemical behaviour of $LiMn_2O_4$. Magnesium was selected as the substitute material because of it low atomic weight compared with $LiMn_2O_4$. The cycling behaviour and ac impedance of a $LiMg_yMn_{2-y}O_4$/Li cell is investigated.

2. Experimental

$LiMg_yMn_{2-y}O_4$ samples were synthesised by reacting a stoichiometric mixture of $LiOH{\cdot}H_2O$ (98+%, Aldrich), MnO_2 (90+%, Aldrich) and MgO (99.95%, Aldrich). The mixture was heated at 800°C for 36 h in air, followed by

* Corresponding author. Tel.: +82-62-530-0740; fax: +82-62-530-0077.
E-mail address: kooroom@hanmail.net (I.-S. Jeong).

0378-7753/01/$ – see front matter
PII: S0378-7753(01)00775-3

grinding in a quartz bowl. The average particle size of the samples was less than 30 μm. Phase analysis of the products was carried out by powder X-ray diffractometry (XRD) using Cu Kα radiation (Dmax/1200, Rigaku Co.). Electrode (cathode) specimens were prepared by mixing the $LiMg_yMn_{2-y}O_4$ power with 15 wt.% sp-270 carbon black and 5 wt.% polyvinylidene fluoride (PVDF). This slurry was pasted on to an aluminium foil. Three-electrode electrochemical cells were employed. The reference and counter electrodes were constructed from lithium foil and 1 M $LiClO_4$-propylene carbonate (PC) solution (Merck) was used as the electrolyte. The cells were assembled in an argon-filled glove box. The charge–discharges cycle performance was examined between 3.0 and 4.3 V with a constant current density of 0.1 mA/cm^2. Impedance spectroscopy was measured in the frequency range 5 mHz–2 MHz with a superimposed amplitude of 10 mV (IM6, Zanher Electrik Co.). The numerical values of the diffusion coefficient from the Warburg region we calculated [11,12] using the following relationship:

$$D = \frac{1}{2}\left[\left(\frac{Vm}{FSA}\right)\left(\frac{dE}{dx}\right)\right]^2 \quad (1)$$

where A is obtained from the Warburg impedance $Z_w = A\omega^{-1/2} - JA\omega^{-1/2}$; $\omega = 2\pi f \gg 2D/L^2$, V_m the oxide molar volume, F the Faraday constant, S the geometric surface area, dE/dx the slope of the coulometric titration curve at each x value. Construction of the cell for ac impedance measurements was similar to that used for charge–discharge studies.

3. Results and discussion

X-ray diffraction (XRD) patterns of $LiMg_yMn_{2-y}O_4$ ($y = 0.00$, 0.05, 0.08, 0.10, 0.12 and 0.15) are indicative of a single-phase spinel with a space group *Fd3m*, in which lithium ions and substituted metal cations occupy tetrahedral (8a) sites and octahedral (16d) sites, respectively.

In Fig. 1 the relationship between the charge and discharge capacity of the cathode and the cycle number is shown for $LiMg_yMn_{2-y}O_4$/Li cells with a 1 M $LiClO_4$-PC electrolyte. A constant current density of 0.1 mA/cm^2 was used. The initial capacity of the cells was reduced by increasing the Mg content in $LiMg_yMn_{2-y}O_4$. The initial discharge capacity of an electrode based on $LiMn_2O_4$ was 118 mAh/g, which decreased rapidly to 75 mAh/g after 50 cycles. The substituted spinels display better cycle performance in terms of capacity and cycle-life compared with $LiMn_2O_4$. For example, the discharge capacity of $LiMg_{0.1}Mn_{1.9}O_4$ is 120 mAh/g on the first cycle and 105 mAh/g at the 70th cycle. The capacity loss during 70 cycles is about 12% of the initial capacity. This behaviour is probably due to the substitution of some M–O linkages in the spinel by Mg–O and the light atomic weight of Mg. Li et al. [13] have reported that doped metal cations

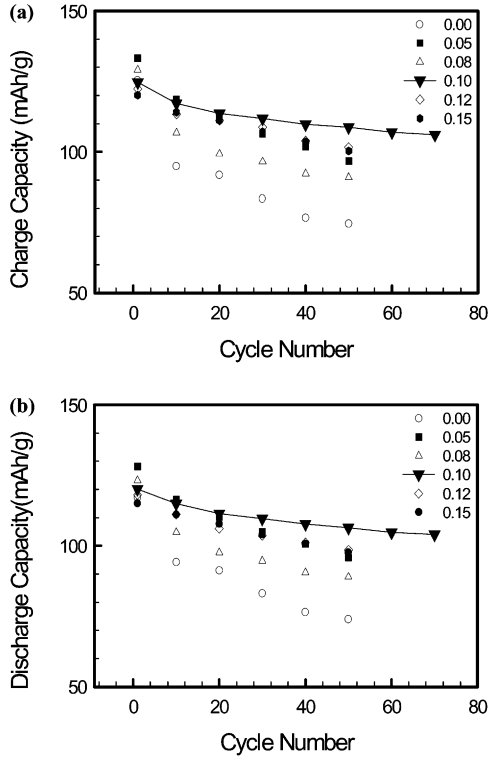

Fig. 1. (a) Charge capacity; (b) discharge capacity of $LiMg_yMn_{2-y}O_4$/Li cells as a function of cycle number. Values of y as shown.

enhance the stability of the octahedral sites in the spinel skeleton structure.

The discharge curves on the first cycle of $LiMg_yMn_{2-y}O_4$/Li cells in the voltage range 3.0–4.3 V are given in Fig. 2. Two voltage plateaux are observed for all cathodes; the plateaux at 4.15 V corresponds to a two-phase reaction and that at 4.01 V to a one-phase reaction [14]. The substituted spinels were discharged from 4.2 V, but the pure spinel from 4.15 V. This is due to the *IR* drop by the high impedance of the $LiMn_2O_4$ cathode compared with the lower impedance of the Mg-substituted cathodes.

The discharge curves at the first cycle, the 50th cycle and the 70th cycle of the $LiMg_{0.1}Mn_{1.9}O_4$/Li cell are shown in

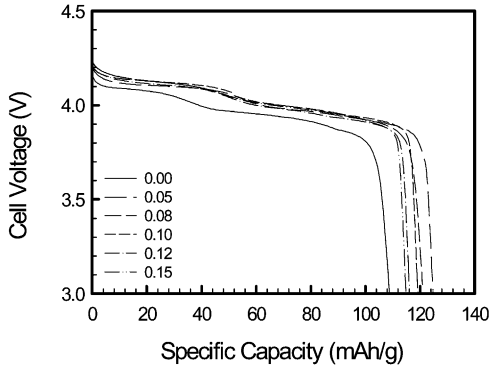

Fig. 2. First discharge curves of $LiMg_yMn_{2-y}O_4$/Li cells.

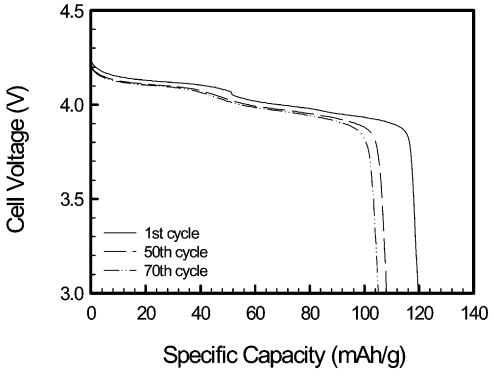

Fig. 3. Discharge curves of $LiMg_{0.1}Mn_{1.9}O_4$/Li cells as a function of cycling.

Fig. 3. The respective discharge capacities are 120, 108 and 105 mAh/g. The discharge capacity at the 70th cycle is about 88% of the initial discharge capacity. A distinct plateau is also observed after the 70th cycle. In addition, the starting point of the discharge at the 70th cycle is nearly the same as that at the first cycle.

In order to investigate the performance of $LiMn_2O_4$/Li and $LiMg_yMn_{2-y}O_4$/Li cells, the ac impedance spectra were measured with charge–discharge cycling. In particular, the $LiMg_{0.1}Mn_{1.9}O_4$/Li cell which showed better cycle performance compared with the others were studied in detail.

The initial impedance spectra and data on the $LiMg_yMn_{2-y}O_4$/Li cells before cycling are given in Fig. 4. The electrolyte resistance of all cells is about 32–35 Ω.

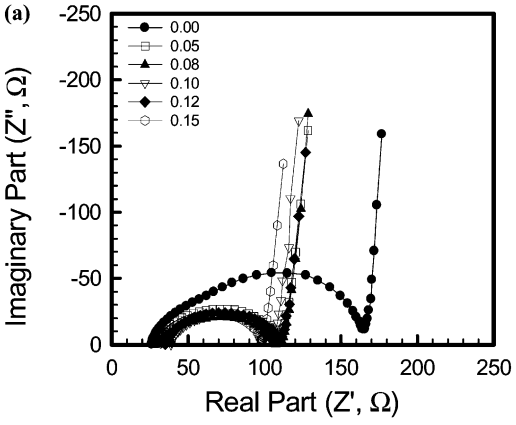

(b)

	Rs	Rct	Cs	Hs	D
0.00	33Ω	135.43Ω	76267.4μF	17.1μH	2.2×10^{-9}
0.05	32Ω	80.57Ω	35112.5μF	13.8μH	6.8×10^{-8}
0.08	33Ω	77.14Ω	21366.5μF	12.8μH	7.2×10^{-8}
0.10	34Ω	65.61Ω	22794.4μF	14.3μH	8.2×10^{-8}
0.12	33Ω	74.55Ω	16463.1μF	12.6μH	5.4×10^{-8}
0.15	35Ω	66.07Ω	28880.6μF	13.3μH	8.0×10^{-8}

Fig. 4. Initial impedance spectra and data of $LiMg_yMn_{2-y}O_4$/Li cells before cycling with (a) the impedance spectra; (b) the impedance data.

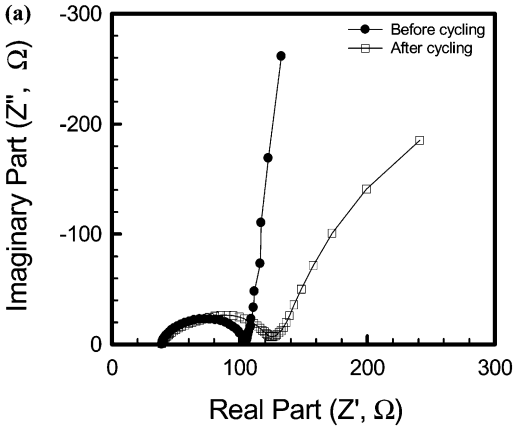

(b)

	Rs	Rct	Cs	Hs	D
Before cycling	34Ω	65.61Ω	22794.4μF	14.3μH	8.2×10^{-8}
After cycling	35Ω	100.14Ω	97078.0μF	11.6μH	9.3×10^{-12}

Fig. 5. Impedance spectra and data on the $LiMg_{0.1}Mn_{1.9}O_4$/Li cells before/after cycling: (a) impedance spectra; (b) the impedance data.

The initial charge-transfer resistance of the $LiMn_2O_4$ cathode is about 135 Ω. By contrast, the value for the substituted cathodes is about 70 Ω. The impedance profiles of the substituted cathodes are more stable than those of the pure cathode. In addition, the substituted cathodes show chemical diffusion coefficients of lithium ions of 10^{-8} cm^2 s^{-1}, and the pure cathode shows 10^{-9} cm^2 s^{-1}. These impedance profiles support the cycle performance reported in Fig. 2. It is recognised that impedance profiles are key factors in cycle performance.

The impedance spectra and data for $LiMg_{0.1}Mn_{1.9}O_4$/Li cells before and after cycling are presented in Fig. 5. The electrolyte resistance does not change, but the charge-transfer resistance and the capacitance increase to 30 Ω and 70,000 μF, respectively after cycling. The chemical diffusion coefficient of lithium ions decreases by about four orders. Also, the slope of the inclined line that indicates the Warburg impedance in the low frequency range is smaller, which indicates a decrease in the activity of lithium ions.

Charge–discharge curves at the first cycle on (a) a $LiMn_2O_4$/Li cell and (b) a $LiMg_{0.1}Mn_{1.9}O_4$/Li cell and the points of ac impedance spectroscopy measurement are shown in Fig. 6. The open circuit voltage of the cells is 3.25 V, the voltage at the end-of-charge is 4.3 V and the voltage at the end-of-discharge is 3.0 V. In addition the $LiMn_2O_4$/Li cell, has voltage plateaux at 4.03, 4.15, 4.11 and 3.99 V and the $LiMg_{0.1}Mn_{1.9}O_4$/Li cell at 4.05, 4.19, 4.13 and 4.00 V during charge–discharge cycling.

The impedance spectra and data for the $LiMn_2O_4$/Li cell during charge–discharge cycling are shown in Fig. 7. The electrolyte resistance is 36–40 Ω during cycling. The initial

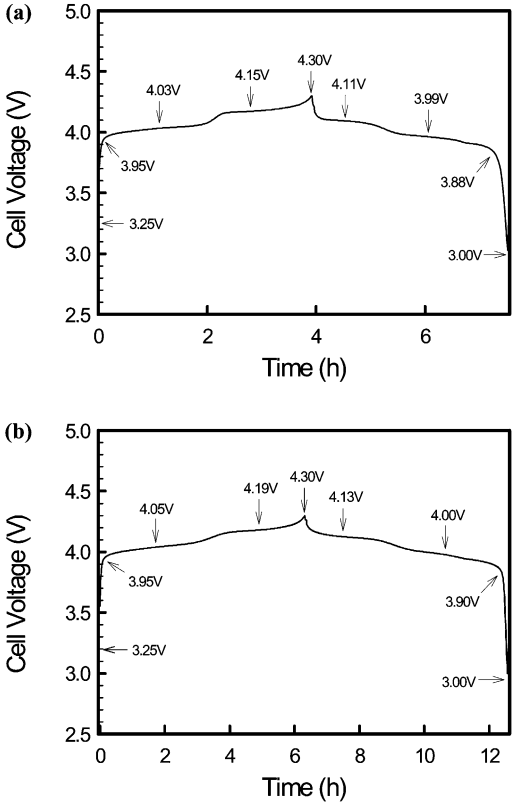

Fig. 6. Charge–discharge curves for first cycle of (a) $LiMn_2O_4$/Li and (b) $LiMg_{0.1}Mn_{21.9}O_4$/Li cell and point of ac impedance spectroscopy measurement.

charge-transfer resistance and the capacitance are 110 Ω and 52,000 μF, respectively. The resistance and the capacitance gradually decrease with charge. By contrast, the impedance spectra for the discharging reaction exhibit the exact reverse behaviour, i.e. the resistance and capacitance gradually increase with discharging. The inductance was however, almost constant with charge–discharge cycling. The variation of the chemical diffusion coefficient of lithium ion is unique. The diffusion coefficient measured at the two voltage plateaux on charging and discharging is about 1–2 orders of magnitude lower than at other points. At present, we are unable to precisely explain this behaviour. Probably, a phase change at the plateau range will prevent lithium ion from diffusing.

The impedance spectra and data on for the $LiMg_{0.1}Mn_{1.9}O_4$/Li cell during charge–discharge cycling are given in Fig. 8. The variation of the impedance spectra for the $LiMg_{0.1}Mn_{1.9}O_4$/Li cell is consistent with that for the $LiMn_2O_4$/Li cell. The impedance gradually decreases with charging and increases with discharging. The inductance and the electrolyte resistance are almost constant during charge–discharge cycling. As shown in Fig. 8(b) and (d) however, the charge-transfer resistance and the capacitance of the $LiMg_{0.1}Mn_{1.9}O_4$/Li cell are smaller and the diffusion coefficient is higher than that of the $LiMn_2O_4$/Li cell. This behaviour suggests that Mg-substitution enhances the impedance stability of $LiMg_yMn_{2-y}O_4$. This agrees with the observed cycle performance. This fact means that the impedance stability of $LiMg_yMn_{2-y}O_4$ due to Mg-substitution

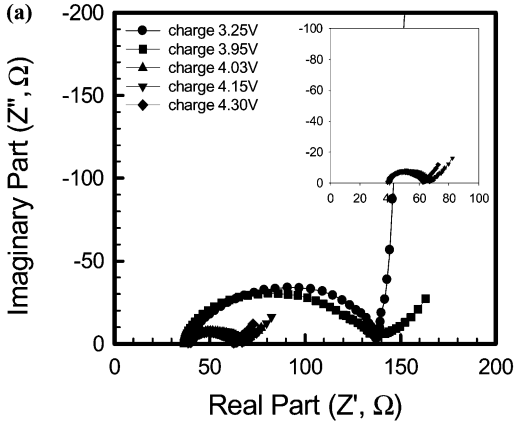

(b)

	Rs	Rct	Cs	Hs	D
3.25V	37Ω	109.25Ω	52016.5μF	12.0μH	8.0×10^{-9}
3.95V	36Ω	108.89Ω	29395.8μF	11.9μH	3.0×10^{-9}
4.03V	38Ω	23.84Ω	5642.1μF	12.2μH	9.8×10^{-10}
4.15V	38Ω	23.47Ω	7223.8μF	12.0μH	2.6×10^{-10}
4.30V	40Ω	23.02Ω	3526.4μF	12.5μH	1.1×10^{-8}

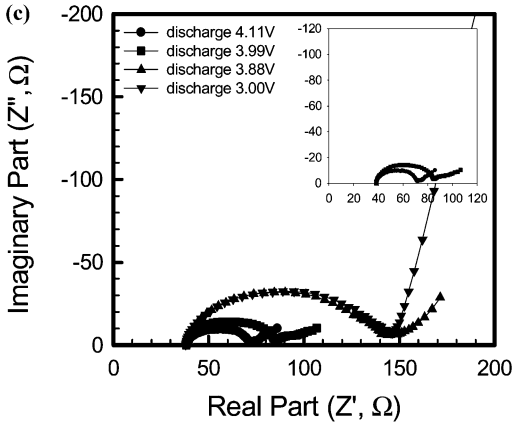

(d)

	Rs	Rct	Cs	Hs	D
4.11V	38Ω	33.57Ω	7271.6μF	12.1μH	2.8×10^{-10}
3.99V	38Ω	47.35Ω	8025.2μF	12.4μH	9.2×10^{-10}
3.88V	37Ω	110.50Ω	30247.4μF	12.7μH	2.1×10^{-9}
3.00V	38Ω	110.57Ω	38848.2μF	12.3μH	1.3×10^{-9}

Fig. 7. Impedance spectra and data for $LiMn_2O_4$/Li cell during charge–discharge cycling: (a) impedance spectra for charging; (b) impedance data for charging; (c) impedance spectra for discharging; (d) impedance data for discharging.

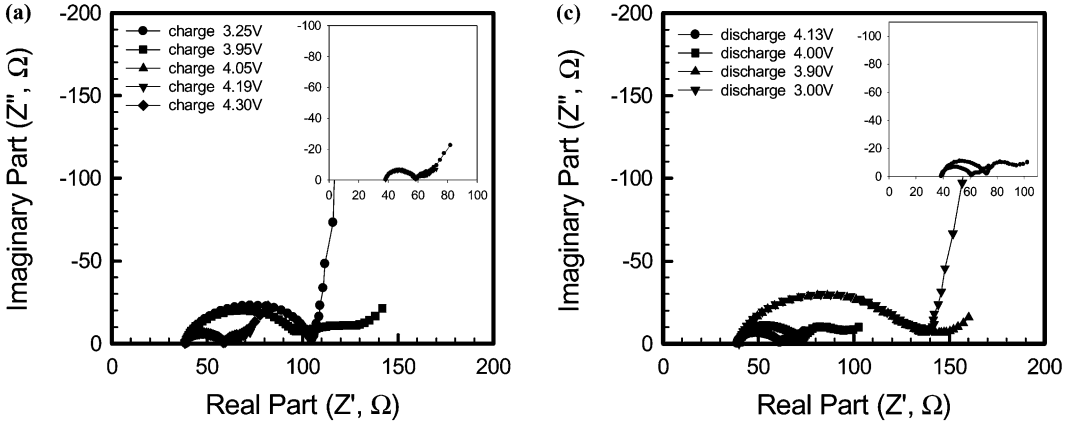

(b)

	Rs	Rct	Cs	Hs	D
3.25V	36Ω	66.81Ω	23614.5μF	12.3μH	7.9×10^{-8}
3.95V	36Ω	61.21Ω	19108.0μF	11.8μH	6.7×10^{-8}
4.05V	37Ω	20.27Ω	4234.8μF	13.7μH	5.3×10^{-9}
4.19V	38Ω	20.23Ω	4200.9μF	13.6μH	1.2×10^{-9}
4.30V	38Ω	20.22Ω	4222.3μF	13.5μH	8.6×10^{-8}

(d)

	Rs	Rct	Cs	Hs	D
4.13V	36Ω	18.57Ω	5505.4μF	13.5μH	5.3×10^{-9}
4.00V	37Ω	21.14Ω	6087.1μF	13.7μH	2.7×10^{-9}
3.90V	37Ω	100.6Ω	29955.9μF	13.1μH	7.2×10^{-9}
3.00V	37Ω	100.5Ω	28783.5μF	12.9μH	6.1×10^{-8}

Fig. 8. Impedance spectra and data for $LiMg_{0.1}Mn_{1.9}O_4$/Li cell during charge–discharge cycling (a) impedance spectra for charging; (b) impedance data for charging; (c) impedance spectra for discharging; (d) impedance data for discharging.

contributes to the reversibility of the charge–discharge cycling. The impedance spectra of the $LiMn_2O_4$/Li cell consists of the one semicircular are in the high-frequency range with a charge-transfer resistance and a capacitance, and the inclined line in the low-frequency range with a Warburg impedance which is associated with lithium-ion diffusion. By contrast, the spectra of the $LiMg_{0.1}Mn_{1.9}O_4$/Li cell consists of two semicircular arcs and an inclined line. The reaction mechanism is still unknown. It is considered, however, that the second arc is probably related to the reaction at the electrolyte/oxide electrode interface by Mg cations substituted for Mn.

4. Conclusions

$LiMg_yMn_{2-y}O_4$ samples for lithium-ion batteries have been prepared at 800°C for 36 h in air and their electrochemical behaviour has been investigated. The cycle performance of the Mg-substituted spinel phases is better than that of the pure spinel $LiMn_2O_4$. In particular, the discharge capacity of a $LiMg_{0.1}Mn_{1.9}O_4$/Li cell is about 120 and 105 mAh/g at the first cycle and the 70th cycle, respectively. The discharge capacity at the 70th cycle is more than 88% of that at the first cycle. The impedance profiles of $LiMg_{0.1}Mn_{1.9}O_4$ are more stable than those of pure spinel during charge–discharge cycling. This suggests that the cycle performance of the cathodes is related to the stability of the impedance profiles.

References

[1] M.M. Thackeray, A. de Kock, M.H. Rossouw, D. Liles, R. Bittihn, D. Hoge, J. Electrochem. Soc. 139 (1992) 363.
[2] J.M. Tarascon, E. Wang, F.K. Shokoohi, W.R. Mckinnon, S. Colson, J. Electrochem. Soc. 138 (1991) 2859.
[3] A. de Pasquier, A. Blyr, A. Cressent, C. Lenain, G. Amatucci, J.M. Tarascon, J. Power Sources 81-82 (1999) 54.
[4] J.N. Reimers, J.R. Dahn, J. Electrochem. Soc. 139 (1992) 2091.
[5] T. Ohzuku, A. Ueda, M. Nagayama, J. Electrochem. Soc. 140 (1991) 1862.
[6] R.J. Gummow, A. de Kock, M.M. Thackeray, Solid State Ionics 69 (1994) 59.
[7] R. Bittihn, R. Herr, D. Hoge, J. Power Sources 43-44 (1993) 223.
[8] G. Pistoia, G. Wang, Solid State Ionics 66 (1994) 135.
[9] M. Hosoys, H. Ikuta, M. Wakihara, Solid State Ionics 111 (1998) 153.
[10] G. Pistoia, D. Zane, Y. Zhang, J. Electrochem. Soc. 142 (1995) 2551.
[11] S. Bach, S. Farcy, J.P. Pereira-Ramos, Solid State Ionics 110 (1998) 193.
[12] T. Uchida, M. Wakihara, Electrochemistry 65 (1997) 21.
[13] G. Li, H. Ikuta, T. Uchida, M. Wakihara, J. Electrochem. Soc. 143 (1996) 178.
[14] T. Ohzuku, M. Kitagawa, T. Hirai, J. Electrochem. Soc. 137 (1990) 769.